Progress In Electromagnetics Research Letters, Vol. 42, 65–78, 2013

ON THE USE OF METAL GRATINGS TO REDUCE DIFFRACTION FROM A FINITE GROUND PLANE IN CIRCULARLY-POLARIZED MICROSTRIP ARRAYS

Adrianus B. Smolders*, Rob M. C. Mestrom, Abolghasem Zamanifekri, and Ad C. F. Reniers

Electromagnetics Group, Department of Electrical Engineering, Eindhoven University of Technology, P. O. Box 513, Eindhoven 5600 MB, The Netherlands

Abstract—It is shown that metal gratings can be used to improve the cross polarization of circularly-polarized aperture-coupled microstrip antennas. The metal gratings reduce edge diffraction from the finite-size grounded dielectric slab on which the antennas are printed. The edge diffraction is due to surface waves that can propagate in the grounded dielectric slab. The design of the metal grating is based on an analytical model, which results in a first-order estimation for the design of the metal grating structure. The model provides physical insight and appears to be accurate enough for the application. Using this model, a prototype was developed, consisting of a circularly-polarized 2×2 microstrip array with associated feeding network. Measurements show that the axial ratio can be reduced down to 1.75 dB within the beam width of the antenna.

1. INTRODUCTION

Many future applications operating at microwave or mm-wave frequencies require high-quality circular polarization. At these frequencies, the propagation channels rely mainly on line-of-sight communication. Circular polarization ensures robust communication, since an accurate polarization alignment is not required for portable and mobile devices. One of these applications is two-way satellite communication for TV and internet access (VSAT), operating at 20 GHz (downlink) and 30 GHz (uplink), see [1]. This application puts strict requirements on the polarization purity of the antenna:

Received 2 July 2013, Accepted 15 August 2013, Scheduled 25 August 2013

* Corresponding author: Adrianus Bernardus (Bart) Smolders (a.b.smolders@tue.nl).

the maximum allowable cross-polar level is −20 dB, corresponding to a maximum Axial Ratio (AR) of only 1.75 dB. Many applications also require electronic beam steering capabilities. Therefore, a focal-plane array concept is considered as the most promising system concept in terms of performance and cost. Since an array is used to illuminate a large reflector in this case, the AR needs to be very low over a relative large region of the main beam of the array or of a sub-array.

When looking at printed antennas, circular polarization can be obtained in several ways. The most straightforward way is illustrated in Figure 1(a), where two feeds with a 90° phase shift are used to excite a single printed antenna, e.g., a circularly-polarized (CP) aperture-coupled microstrip antenna (ACMA) as reported in [2, 3]. An alternative method is shown in Figure 1(b). It uses sequentially-rotated linearly polarized (LP) antenna elements in an array configuration [4–6].

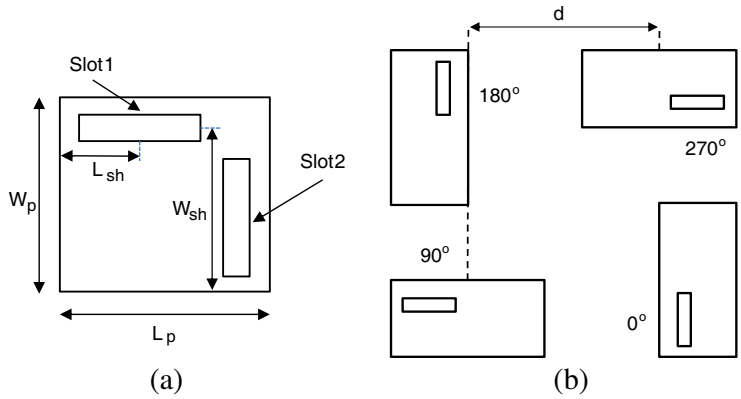

Figure 1. Top views of (a) single circularly-polarized aperture-coupled microstrip antenna (ACMA), (b) circularly-polarized 2×2 array using sequentially-rotated linearly-polarized ACMA antennas.

The design of circularly-polarized printed antennas requires a trade-off between various specifications. Next to a low AR, most applications also require a wide bandwidth, resulting in the use of electrically thick substrates for the printed antennas. An approach to improve the AR for circularly-polarized microstrip antennas is to exploit the symmetry of the structure. To illustrate this, let us consider the characteristics of the square antenna of Figure 1(a), designed for an operating frequency around 6 GHz. Figure 2 shows the corresponding predicted AR of this antenna, which indicates poor circular polarization properties due to the asymmetry of the feed

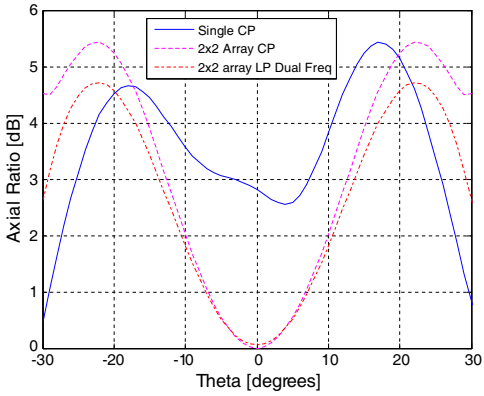

Figure 2. Calculated axial ratio of a single CP element compared to a 2×2 array of CP elements and a 2×2 array of LP dual-polarized elements, $f = 6\,\text{GHz}$, $\varphi = 0°$ plane. ACMA radiators are used with $W_p = L_p = 10.2\,\text{mm}$, $L_{sh} = 3.7\,\text{mm}$, $W_{sh} = 8.7\,\text{mm}$ (CP element) and $W_p = 10.2\,\text{mm}$, $L_p = 17.5\,\text{mm}$, $L_{sh} = 4.2\,\text{mm}$, $W_{sh} = 6.7\,\text{mm}$, $d = 35\,\text{mm}$ (LP elements), slot size is $9.3 \times 1.5\,\text{mm}^2$. The antennas are printed on a grounded dielectric slab with $\varepsilon_r = 3.55$, $h = 3.048\,\text{mm}$ and ground plane size of $150 \times 150\,\text{mm}^2$. Simulations are done with a Finite Integration Technique [23].

configuration. The polarization can be improved by improving the symmetry of the feeding structure [3] or by using the CP element of Figure 1(a) in a 2×2 sub-array configuration and employing sequential rotation of the elements [7, 8]. This results in a more symmetrical configuration and, as a result, in improved polarization properties, as shown in Figure 2. In the simulation, a finite ground plane was used. Circular polarization can also be generated by using LP elements with sequential rotation. Based on this, a shared-aperture concept has recently been introduced in [9], in which a circularly-polarized 2×2 sub-array of ACMA radiators was designed to operate at two frequencies simultaneously. The reported AR of this array is also shown in Figure 2. Note that the 3 dB beam width of both arrays of Figure 2 is approximately 31°. The predicted AR in the $\varphi = 0°$ plane of the LP configuration on a finite ground plane is somewhat better than the 2×2 array of CP elements, due to the absence of coupling between the horizontal and vertical slots. Although both arrays show a low AR at broadside ($\theta = 0°$), the AR is deteriorated significantly for off-broadside angles. Therefore, both configurations do not meet the strict AR requirement of 1.75 dB within the 3 dB beam

width ($-15.5^\circ < \theta < 15.5^\circ$). The degradation of the AR is due to diffraction from the finite-size grounded dielectric slab on which the patches have been printed.

As reported in [9–14], surface-wave propagation in electrically thick substrates deteriorates the antenna gain and affects the radiation characteristics. In [10] it has already been shown that electromagnetic bandgap (EBG) structures can reduce the effect of surface waves on the antenna gain significantly. The purpose of this paper is to extend this idea to the case of improving the polarization quality of circularly-polarized microstrip sub-arrays that employ sequential rotation and are printed on a relative thick, finite-size, grounded dielectric slab. This is achieved by creating a bandgap by applying the very basic EBG structure of metal gratings, resulting in a strong attenuation of the propagating surface-wave modes. In this way, the spurious radiation from the edges of the finite dielectric slab will be reduced, yielding an improved AR. We will use an analytic equivalent-circuit representation to obtain the optimal dimensions of the layout of the metal grating structure. The dispersion equation of the structure is represented in terms of an equivalent network of parallel impedances, which provides physical insight and allows for easy implementation in a circuit simulator. It should be noted that our approach does not require any shorting pins, thus reducing the overall cost of the required technology. The EBG structure which was reported in [12] for the case of a single microstrip antenna, does require shorting pins.

This paper is organized as follows: Sections 2 and 3 are devoted to the metal grating EBG structure. In Section 2, the equivalent circuit model and the dispersion characteristics of a two-dimensional metal grating structure on a grounded dielectric slab are described. In Section 3, based on the equivalent circuit model, we describe the optimization of the metal grating for application to the 2×2 circularly polarized sub-array considered in our work. Next, in Section 4, we describe experimental results of the metal grating structure for a 2×2 antenna sub-array prototype operating at 6 GHz and we compare these to simulations. Finally, some conclusions will be given in Section 5.

2. METAL GRATINGS ON A GROUNDED DIELECTRIC SLAB

The geometry under investigation is shown in Figure 3. The two-dimensional (2D) structure consists of metal gratings placed on top of a grounded dielectric slab with a relative permittivity ε_r. In this paper we will neglect dielectric losses. The periodicity and the width of the metal strips are indicated by l and l_g, respectively.

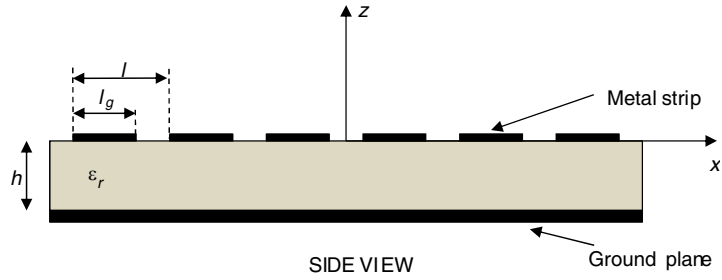

Figure 3. Metal grating on a grounded dielectric slab.

In [10] it was shown that the structure of Figure 3 has bandgap properties for the fundamental Transverse Magnetic (TM_0) mode. Our goal here is to develop a relatively simple, but accurate, equivalent-circuit model for solving the dispersion equation. Starting point of our model is the work that was done in [15, 16], in which the so-called "sampling method" is used to derive an expression for the fields due to a magnetic line source, placed above the metal grating. This formulation assumes that the fields along the slots between the metal strips are constant and therefore this formulation only holds for the case of narrow slots, i.e., $l_g - l < \lambda_\varepsilon/(2\pi)$ with λ_ε the wavelength in the dielectric slab. Extensions to the more general case have been reported in [17–19]. As we will see later, using only narrow slots does not introduce major design limitations for the intended application. The poles of the obtained spectral-domain Green's function correspond to the complex propagation constants of the modes that can propagate in the structure. We have re-formulated the approach of [15, 16] in a more convenient way. It turns out that the dispersion equation can be determined by means of the equivalent circuit representation of Figure 4, similar to the network formulation as reported in [20, 21]. This results in a very compact and physical representation of the dispersion equation. The impedances Z_n, which correspond to the n-th harmonic TM-mode in the z-direction, can be represented by the equivalent transmission-line circuit of Figure 5.

The complex propagation constant k of a guided wave along the periodic grating structure (x-direction) can now be determined from the equivalent circuit of Figure 4, resulting in the following transverse resonance equation:

$$\frac{1}{Z_s} + \sum_{n=-\infty}^{\infty} \frac{1}{Z_n} = 0, \tag{1}$$

where the equivalent mode impedances Z_n and the equivalent surface

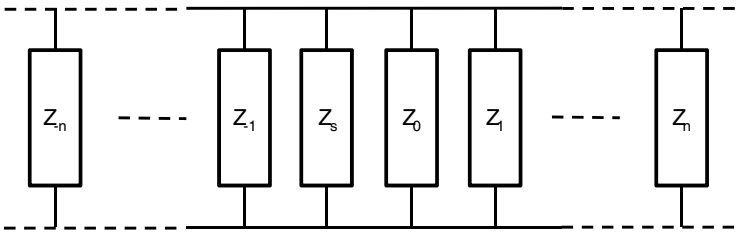

Figure 4. Equivalent circuit representation for determining the dispersion characteristics of surface waves of a metal grating on a grounded dielectric slab.

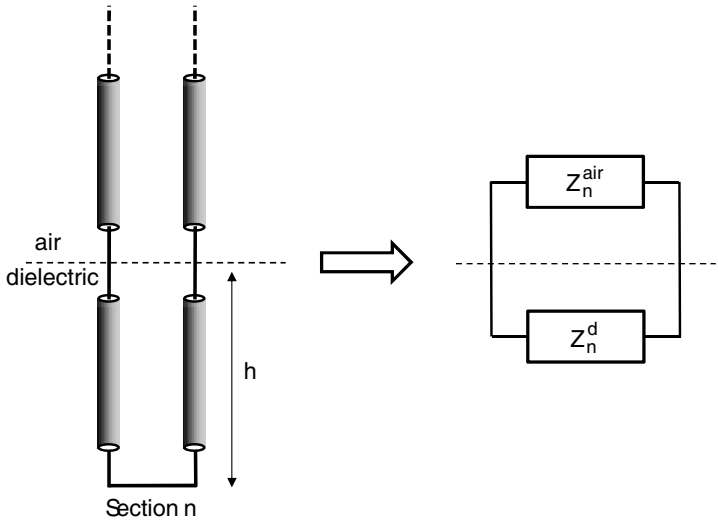

Figure 5. Equivalent z-transmission line circuit of section n.

impedance Z_s are given by:

$$\begin{aligned}
\frac{1}{Z_n} &= \frac{1}{Z_n^{air}} + \frac{1}{Z_n^d}, \\
Z_n^{air} &= \frac{\eta_0 p_n^{(1)}}{k_0}, \\
Z_n^d &= \frac{j\eta_0 p_n^{(2)} \tan\left(p_n^{(2)} h\right)}{\varepsilon_r k_0}, \\
Z_s &= \frac{1}{Y_{s0} + Y_{s1}}
\end{aligned} \tag{2}$$

$$
\begin{aligned}
Y_{s0} &= -\frac{(\varepsilon_r+1)}{\pi}\left(\frac{jlk_0}{\eta_0}\right)\left(\ln\left(\frac{2\pi\,(l-l_g)}{l}\right)-1.5\right),\\
Y_{s1} &= \sum_{n=1}^{\infty}\frac{(\varepsilon_r+1)\,k_0 l}{j\eta_0\pi n},\\
p_n^{(1)} &= \sqrt{k_0^2-k_n^2},\\
p_n^{(2)} &= \sqrt{\varepsilon_r k_0^2-k_n^2},\\
k_n &= k+\frac{2\pi n}{l}.
\end{aligned}
$$

In (2), k is the complex propagation constant of a particular mode along the periodic grating structure, and k_0 and η_0 represent the wave number and wave impedance in free-space. Z_n^{air} represents the wave impedance of the n-th TM-mode in air (region 1), and Z_n^d is the equivalent impedance of the n-th TM-mode in the grounded dielectric of height h (region 2). The propagation constants of the n-th mode in the z-direction in both regions are given by $p_n^{(1)}$ and $p_n^{(2)}$, respectively. Note that in [16], a factor l/ε_r is missing in the expression corresponding to Z_o^d in (2). The equivalent network representation with a simple analytical representation of the dispersion equation allows for easy implementation in standard design tools, since only a limited number of terms need to be taken into account for most practical configurations. In addition, the representation gives additional physical insight into the modeling of the metal grating structure. We solved the non-linear dispersion Equation (1) with a trust-region method [22]. We verified our implementation of the model with the results from rigorous modeling from [10]. Using parameters $\varepsilon_r = 10$, $h = 5\,\text{mm}$, $l = 30\,\text{mm}$ and $l_g = 25\,\text{mm}$, an error of less than 5% was obtained for the estimate of the start frequency of the bandgap region. From Section 4, it will become clear that this accuracy is sufficient for the design of the metal grating structure in our work.

3. OPTIMIZATION OF THE METAL GRATING

The configuration considered in our work is the same as shown in Figure 3, having $\varepsilon_r = 3.55$ (Rogers 4003) and $h = 3.048\,\text{mm}$. For the proof of principle, a center frequency of operation of $f_0 = 6\,\text{GHz}$ will be used. At this frequency, only the fundamental TM_0 mode can propagate in the structure. The thickness of the dielectric slab is approximately $0.11\lambda_d$, where $\lambda_d = \lambda_0/\sqrt{\varepsilon_r}$ is the wavelength in the dielectric. We have done a parameter study to determine the optimal

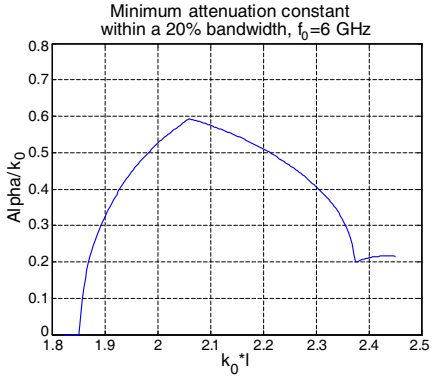

Figure 6. Minimum normalized attenuation constant α/k_0 with in a 1.2 GHz (20%) band around the center frequency $f_0 = 6$ GHz, with $\varepsilon_r = 3.55$, $h = 3.048$ mm and $l - l_g = 3$ mm.

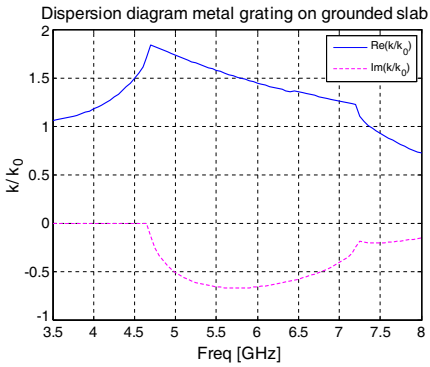

Figure 7. Dispersion diagram of metal grating on a grounded dielectric slab, with $\varepsilon_r = 3.55$, $h = 3.048$ mm, $l = 17$ mm and $l_g = 14$ mm.

bandgap performance by solving (1) for the complex propagation constant k. In Figure 6, the normalized minimum attenuation constant $\alpha/k_0 = \mathrm{Im}\{k\}/k_0$ within a 20% bandwidth around the center frequency f_0 is plotted versus the normalized grid spacing. The discontinuity at the peak is related to whether the lowest $(0.9f_0)$ or highest frequency $(1.1f_0)$ limits the attenuation. We have selected $k_0 l = 2.1$ as the design value for the grid spacing in the prototype, to achieve an attenuation near the peak in the curve of Figure 6.

By choosing $l = 17$ mm and $l_g = 14$ mm, we have obtained a bandgap behavior as shown in Figure 7. The stop-band starts when $k = \pi/l$, corresponding to $k/k_0 = 1.84$. The bandwidth of the stop-band is more than 30%, which is more than required for the targeted applications. The attenuation constant at 6 GHz is $\alpha = 0.66k_0$. This implies that the metal grating structure provides an attenuation of the TM_0 mode of -12.3 dB over one grating period of 17 mm. Therefore, only a limited number of strips are needed to provide sufficient attenuation.

In order to verify the effect of the metal grating structure, the following simulation has been performed. We have compared the mutual coupling between two horizontally-polarized ACMAs printed on the grounded dielectric slab with and without metal grating structure between the antennas. For this purpose, we have used the Finite Integration Technique (FIT) [23]. Figure 8 shows the coupling

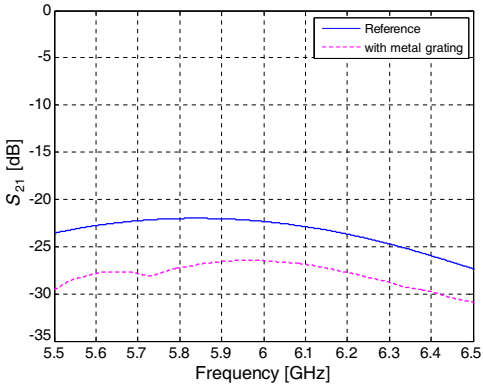

Figure 8. Mutual coupling S_{21} between two aperture-coupled microstrip antennas. Results are shown for the cases without and with metal gratings with parameters: $l_g = 14\,\text{mm}$, $l = 17\,\text{mm}$. Other parameters are $\varepsilon_r = 3.55$, $h = 3.048\,\text{mm}$ and $f = 6\,\text{GHz}$.

coefficient S_{21} between both antennas for the optimized metal grating structure, with only three metal strips between both antennas. The ACMA antenna size is in this case $W_p \times L_p = 17.5 \times 10.2\,\text{mm}^2$ and the center-to-center distance between both antennas is 98 mm. For comparison, the coupling without metal gratings is also shown. The metal grating parameters are $l_g = 14\,\text{mm}$, $l = 17\,\text{mm}$. Clearly, the metal gratings reduce the propagation of the TM_0 mode, since the propagation constant k is complex with $\text{Im}\{k\} < 0$. The coupling is reduced by more than 4 dB in the frequency band of interest ($S_{11} < -10\,\text{dB}$ for $5.7 < f < 6.2\,\text{GHz}$).

4. EXPERIMENTAL VERIFICATION

In order to verify the effect of the metal gratings a prototype was realized, operating at 6 GHz. This relative low frequency was chosen for the proof of principle and for avoiding manufacturing and measurement issues, which might occur when using much higher frequencies. Figure 9 shows the configuration and corresponding dimensions of the prototype.

The array consists of four sequentially-rotated, linearly-polarized, ACMA antennas, generating Left-Hand-Circular (LHC) polarization. The array is fed by a microstrip Wilkinson feed network that generates equal amplitudes and the required phase according to the sequence of Figure 9. The main beam of the array is directed towards broadside.

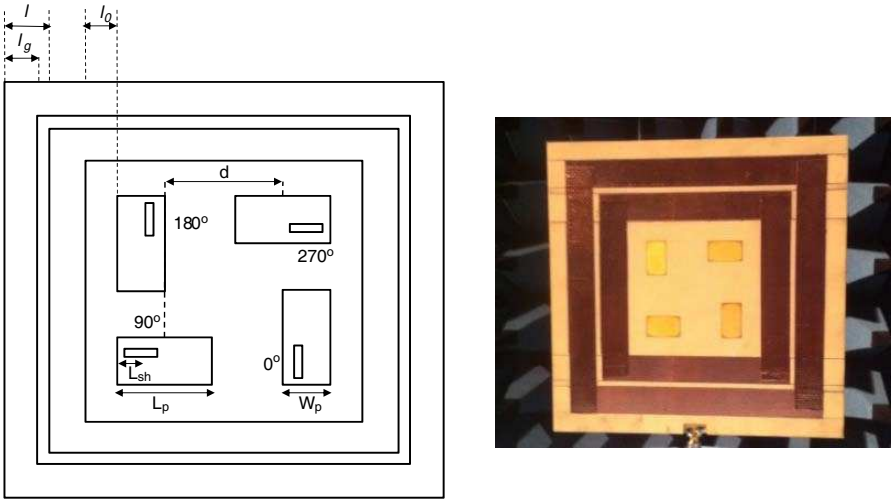

Figure 9. Schematic layout and a picture of the prototype with two metal grating rings to verify the effectiveness of metal gratings to reduce the effect of the finite ground plane on the axial ratio of a 2 × 2 array of ACMA antennas. Dimensions are: $l_g = 14\,\text{mm}$, $l = 17\,\text{mm}$, $l_0 = 10\,\text{mm}$, $L_p = 17.5\,\text{mm}$, $W_p = 10.2\,\text{mm}$, $L_{sh} = 4.2\,\text{mm}$, $W_{sh} = 6.7\,\text{mm}$ and $d = 35\,\text{mm}$. The slot size is $9.3 \times 1.5\,\text{mm}^2$, $\varepsilon_r = 3.55$ and $h = 3.048\,\text{mm}$.

The slots are coupled to 50 Ohm microstrip lines. The microstrip feed network is integrated on the back-side of the microstrip array. The input matching bandwidth ($S_{11} < -10\,\text{dB}$) of the individual ACMA antennas is approximately $+/-5\%$ around the center frequency. Two metal grating rings are used to suppress surface-wave propagation, which were observed to be a cause for edge diffraction in [9]. The dimensions of the grating structure were obtained from the analytical model, as discussed in Section 3. From Figure 9 it can be seen that the overall size of the antenna is increased significantly due to the metal grating structure, similar to the size increase of the EBG prototypes in [10, 12]. However, most applications will require a large number of array elements. In this case, the relative area occupied by the metal gratings will reduce significantly. The measured return loss of the complete 2×2 array with Wilkinson feed network is shown in Figure 10.

The measured and simulated AR, with and without the metal gratings, are shown in Figure 11 in the $\varphi = 0°$ plane. In both cases, the ground-plane size is $150 \times 150\,\text{mm}^2$. The simulation of the complete structure was done with a FIT technique [23]. From Figure 11 we can

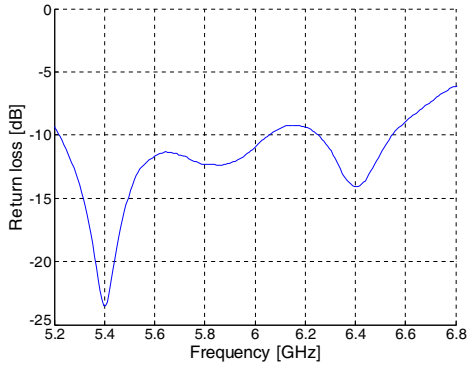

Figure 10. Measured return loss of the circularly-polarized prototype of Figure 9 with feed network.

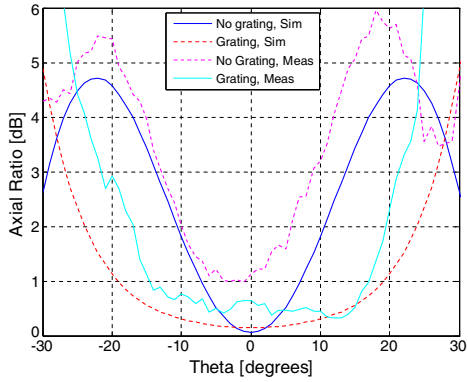

Figure 11. Measured and calculated AR of the circularly-polarized prototype of Figure 9 with and without metal gratings, $f = 6\,\text{GHz}$, $\varphi = 0^\circ$ plane, θ step size measurements 1°. The ground-plane size is $150 \times 150\,\text{mm}^2$ in all cases.

conclude that the metal gratings clearly reduce the effect of diffraction at the edges of the finite grounded dielectric slab. The AR is reduced significantly and is below 1.75 dB within the entire beam width of the 2×2 sub-array. Note that the 3-dB beam width of the co-polarized beam is approximately 31°. Furthermore, as observed from Figures 6 and 7, the attenuation of the surface waves should be relative constant over a wide frequency range. This is confirmed by the measured AR of the prototype with metal grating structure for three different frequencies, which are shown in Figure 12.

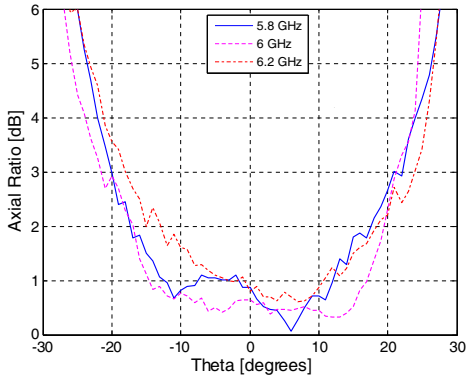

Figure 12. Measured AR of the prototype with metal gratings of Figure 9 for various frequencies, $\varphi = 0°$ plane, θ step size measurements 1°.

5. CONCLUSION

In this paper we have shown that the effect of diffraction of a finite ground plane on the axial ratio of circularly-polarized microstrip antennas can be reduced significantly by using metal gratings. The proposed analytical model for describing the surface-wave modes in the grounded dielectric slab with metal gratings provides an excellent design guideline for the grating structure. The experimental results from a 6 GHz prototype with metal gratings confirm the reduction of diffraction from the finite-size grounded dielectric slab. As a result, the AR is improved significantly. With grating structure, the AR is below 1.75 dB within the 3-dB beam width of the antenna over a sufficiently large frequency range.

ACKNOWLEDGMENT

This work was carried out in the framework of the European CATRENE project "RF2THz".

REFERENCES

1. Dell, J., "The maritime market: VSAT rules," *SatMagazine*, 30–34, Dec. 2008, available on-line: www.satmagazine.com.
2. Adrian, A. and D. H. Schaubert, "Dual aperture-coupled microstrip antenna for dual or circular polarization," *Electronics Letters*, Vol. 23, No. 23, 1226–1228, 1987.

3. Targonski, S. D. and D. M. Pozar, "Design of wideband circularly polarized aperture-coupled microstrip antennas," *IEEE Transactions on Antennas and Propagation*, Vol. 41, No. 2, 214–220, 1993.
4. Huang, J., "A technique for an array to generate circular polarization with linearly polarized elements," *IEEE Transactions on Antennas and Propagation*, Vol. 34, No. 9, 1113–1124, Sep. 1986.
5. Hall, P. S., J. Huang, E. Rammos, and A. Roederer, "Gain of circularly polarized arrays composed of linearly polarized elements," *Electronics Letters*, Vol. 25, No. 2, 124–125, 1989.
6. Smolders, A. B. and U. Johannsen, "Axial ratio enhancement for circularly-polarized millimeter-wave phased-arrays using a sequential rotation technique," *IEEE Transactions on Antennas and Propagation*, Vol. 59, No. 9, 3465–3469, 2011.
7. Baggen, L., S. Holzwarth, W. Simon, and O. Litschke, "Phased array using the sequential rotation principle: Analysis of coupling effects," *IEEE International Symposium on Phased Array Systems and Technology*, 571–576, Oct. 14–17, 2003.
8. Pawlak, H. and A. F. Jacob, "An external calibration scheme for DBF antenna arrays," *IEEE Transactions on Antennas and Propagation*, Vol. 58, No. 1, 59–67, Jan. 2010.
9. Smolders, A. B., R. M. C. Mestrom, A. C. F. Reniers, and M. Geurts, "A shared aperture dual-frequency circularly polarized microstrip array antenna," *IEEE Antennas and Wireless Technology Letters (AWPL)*, Vol. 12, 120–123, 2013.
10. Llombart, N., A. Neto, G. Gerini, and P. de Maagt, "Planar circularly symmetric EBG structures for reducing surface waves in antennas," *IEEE Transactions on Antennas and Propagation*, Vol. 53, No. 10, 3210–3218, 2005.
11. Bolt, R. J., D. J. Bekers, N. Llombart, A. Neto, and G. Gerini, "Application of EBG structures at sub-array level," *Proc. of the 36th European Microwave Conference*, 1052–1055, Sep. 2006.
12. Rahman, M. and M. A. Stuchly, "Circularly polarised patch antenna with periodic structure," *IEE Proceedings — Microwaves, Antennas and Propagation*, Vol. 149, No. 3, 141–146, 2002.
13. Zheng, B. and Z. Shen, "Effect of a finite ground plane on circularly polarized microstrip antennas," *IEEE International Symposium on Antennas and Propagation*, Vol. 2A, 238–241, Jul. 3–8, 2005.

14. Das, N. K. and A. Mohanty, "Infinite array of printed dipoles integrated with a printed strip grating for suppression of cross-polar radiation. I. Rigorous analysis," *IEEE Transactions on Antennas and Propagation*, Vol. 45, No. 6, 960–972, 1997.
15. Sigelmann, R. A. and A. Ishimaru, "Radiation from periodic structures excited by an aperiodic source," *IEEE Transactions on Antennas and Propagation*, Vol. 13, No. 3, 354–364, 1965.
16. Sigelmann, R. A., "Surface waves on a grounded dielectric slab covered by a periodically slotted conducting plane," *IEEE Transactions on Antennas and Propagation*, Vol. 15, No. 5, 672–676, 1967.
17. Bellamine, F. H. and E. F. Kuester, "Guided waves along a metal grating on the surface of a grounded dielectric slab," *IEEE Transactions on Microwave Theory and Techniques*, Vol. 42, No. 7, 1190–1197, 1994.
18. Kaganovsky, Y. and R. Shavit, "Analysis of radiation from a line source in a grounded dielectric slab covered by a metal strip grating," *IEEE Transactions on Antennas and Propagation*, Vol. 57, No. 1, 135–143, 2009.
19. Jacobsen, J., "Analytical, numerical, and experimental investigation of guided waves on a periodically strip-loaded dielectric slab," *IEEE Transactions on Antennas and Propagation*, Vol. 18, No. 3, 379–388, 1970.
20. Maci, S., M. Casaletti, M. Caiazzo, and A. Cucini, "Dispersion analysis of printed periodic structures by using a pole-zero network synthesis," *17th International Conference on Applied Electromagnetics and Communications, ICECom 2003*, 300–303, 2003.
21. Guglielmi, M. and H. Hochstadt, "Multimode network description of a planar periodic metal-strip grating at a dielectric interface. III. Rigorous solution," *IEEE Transactions on Microwave Theory and Techniques*, Vol. 37, No. 5, 902–909, 1989.
22. Sande, H. V., H. de Gersem, F. Henrotte, and K. Hameyer, "Solving nonlinear magnetic problems using Newton trust region methods," *IEEE Transactions on Magnetics*, Vol. 39, No. 3, 1709–1712, 2003.
23. Hirtenfelder, F. and G. Lubkowski, "3D field simulations using FI time domain technique of wedge- and parabolic-shaped left handed materials (LHM)," *International Workshop on Antenna Technology (IWAT)*, 259–262, 2007.